

Geotechnical Design and Construction Challenges of Samuel de Champlain Bridge in Montreal

Diab, Riad, Principal Geotechnical Engineer, Construction Kiewit CIE
Tardif, Jean, Project Director, SNC Lavalin
D'Amours, Louis, Vice President Business Development, SNC Lavalin
LaRoche, Martin, Geotechnical Design Director, Construction Kiewit CIE
Beaulieu, Jean-François, Senior Geotechnical Engineer, Construction Kiewit CIE

Paper prepared for
TESTING AND MODELING OF ROADWAY/
EMBANKMENT MATERIALS AND GEOTECHNICAL ENGINEERING
Session of the 2021 TAC Conference & Exhibition

ABSTRACT

In 2015, the Canadian government awarded a \$4.3 Billion Design-Build contract to the Joint Venture (JV) team “Signature on the Saint Lawrence (SSL)” for the design and construction of one of the largest infrastructure projects in North America, Samuel de Champlain Bridge over Saint-Laurence River between Montreal and Brossard. The complexity of the project posed unique geotechnical challenges on many levels.

One significant challenge was the construction of part of the alignment over an old landfill where the subsurface investigation indicated up to 9 m of solid waste. To assess the foundation material properties, settlement monitoring was performed during the design phase on a 7-m high temporary embankment, constructed on the existing fill, using numerous settlement plates. The “consolidation” and strength parameters were then back-calculated and used in the roadway embankment design.

On the west approach, part of the new highway alignment was to be constructed over an existing 11x5 m COS collector with unknown structural condition, with the requirement not to apply additional load on the collector. Lightweight fill composed of expanded polystyrene was used for this purpose. Detailed numerical analysis of the stress-strain conditions was performed to optimize the design.

Other challenges included designing foundation system in a thick liquefiable silty soil deposit to withstand seismic loading induced during a 2% in 50-year return period. Moreover, the presence of soft clay layer at the east approach roadway where up to 16 m of fill was to be placed led the geotechnical team to perform a detailed settlement analysis that was later compared to settlement monitoring results during construction. Furthermore, the rock formation at the site was known to exhibit relaxation (decrease in resistance) phenomenon for piles driven to refusal on bedrock. A thorough dynamic testing program was developed to carefully assess the nominal pile resistance.

This paper addresses the issues encountered and concerns raised during the geotechnical design and how these were addressed and resolved. Design and construction procedures, challenges and solutions are discussed in detail.

1 INTRODUCTION

The former Champlain Bridge, constructed in 1958, across the St-Lawrence River between Brossard and Montreal required replacement as a result of age and premature critical structural deterioration. The new Champlain Bridge, named Samuel de Champlain, was constructed by a joint venture called Signature on St Lawrence, comprised of SNC Lavalin, Dragados Canada, and ASC Infrastructure, partnering with SNC Lavalin, WSP and T.Y. Lin International as the lead design firms, and was opened to traffic on July 1, 2019. It was one of the largest infrastructure projects in North America and is one of the busiest crossings on the continent.

In addition to the new 3.5 km main bridge, the overall project involved the construction of tens of smaller bridges, including the 8-span, 470 m long, Ile des Sœurs (Nun’s Island) Bridge, and over 20 retaining walls along the bridge approaches. The project also included the widening of highway 15 between the Turcot Interchange and the new bridge, and the improvement of the ramps leading from Highways 132 and 10 on the South Shore (Brossard) to the new bridge. Figure 1 below show the location of the project limits.



Figure 1. Champlain Bridge alignment

The “main” bridge is 39 spans and comprises three consecutive segments: The West Approach, the Cable Stayed Bridge (CSB), and the East Approach (see Figure 2 below). The West Approach (towards Montreal) is 27 spans, 2 km long from IDS to the CSB. The Cable Stayed Bridge (CSB) is approximately 500 m long and crosses the navigation channel of the St. Lawrence Seaway between an existing dike and the Couvée Island Bird Sanctuary. The East Approach is 770 m long and extends from CSB to Brossard Shore with 11 substructures.

The new bridge carries traffic of highways A-10, A-15, and A-20 as well as the South Shore branch of the forthcoming Réseau express métropolitain (REM), a 67 km automated light rail system.



Figure 2. Main bridges segments

As per Transport Canada (client) requirements, the main standards to be used for the geotechnical design over and above the detailed Project Agreement specifications were the Canadian Highway Bridge Design Code (CSA-S6-14), the Canadian Foundation Engineering Manual (CFEM 2006), and AASHTO LRFD Bridge Design Specifications (2014), in decreasing order of precedence. The new bridge design life is 125 years and is classified as lifeline bridge according to S6-14 importance category. The seismic design was to be performed for a return period of 2% in 50-year.

The bridge had to be designed and constructed in a 42-month timeframe. The complexity of the project posed unique geotechnical challenges on many levels. This paper presents some of the design and construction challenges.

2 SITE GEOLOGIC CONDITIONS

The general geology at the site consists of 1 to 4 m of glacial till deposit overlying the bedrock encountered at depths varying between 2 and 12 m. The overburden soil overlying the till is mostly granular fill although clay deposit from the Champlain Sea is encountered on the South Shore. The rock type is shale from the Utica formation. The surface of the bedrock is altered and fractured for depths varying from 1 to 5 m.

3 FOUNDATION TYPE

Although deep foundation system, consisting mostly of drilled shafts socketed into rock, was the most suitable foundation type for supporting the bridges, some of the “main” bridge substructures were supported by spread footings on rock due to the shallow depth of bedrock.

The drilled shaft diameter varied from 0.6 m to 2.2 m with the largest diameters used for the 8-span Ile des Sœurs (IDS) bridge.

The Main Span Tower (MST) is supported by 42 drilled shafts having 1.18 m diameter and socketed about 4 m into sound bedrock as shown on Figure 3 below.

The 28 substructures of the West Approach (towards Montreal), designated as WB (West Abutment), and W01 to W27 are all supported by spread footing on rock (See Figure 4) apart from W01, W02, and WB where 1.18 m diameter drilled shafts were the selected foundation type.

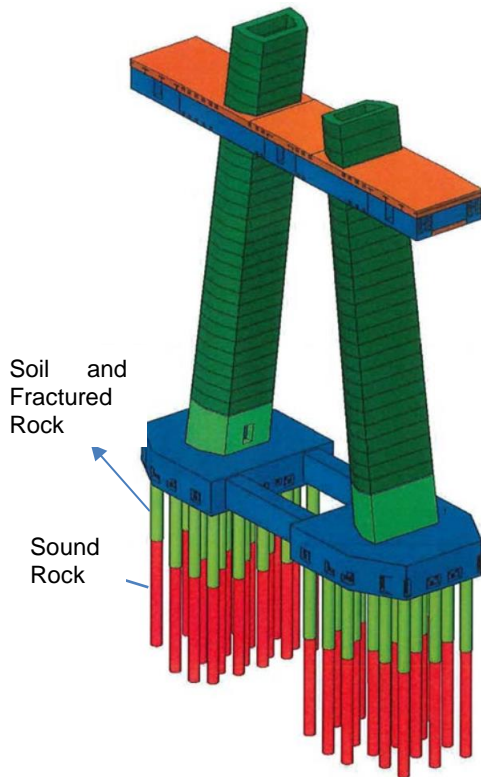


Figure 3. Main Span Tower foundations

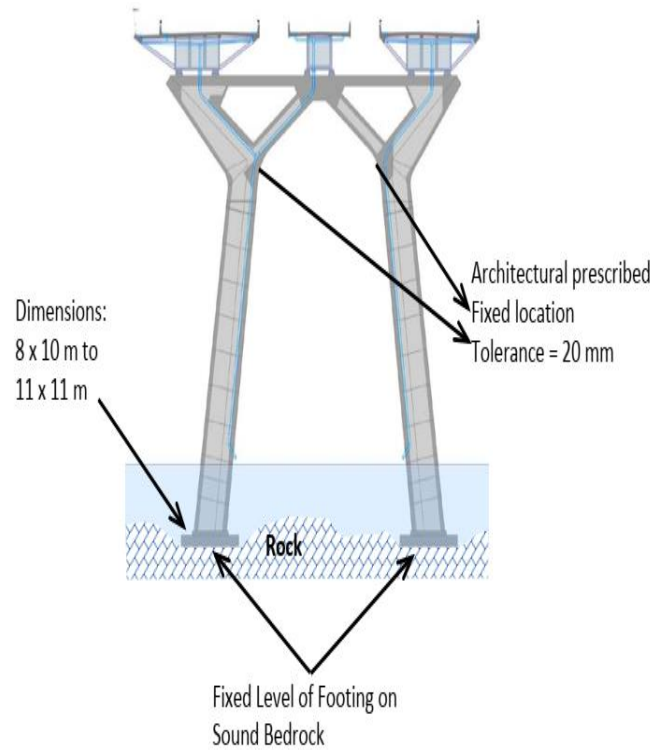


Figure 4. Typical “main” bridge shallow foundation

The foundation types of the East Approach substructures, designated as EB (East Abutment) and E01 through E10, include driven piles, drilled shafts and spread footings. Substructures E02 to E06 are on shallow foundations bearing on rock; EB and E07 are on groups of 1.18-meter diameter drilled shafts; and E08 to E10 on groups of 0.4-meter diameter driven piles.

4 SUBSURFACE INVESTIGATION CHALLENGES

The geotechnical investigation consisted of over 200 borings (including 69 offshore), over 40 Cone Penetration Tests with or without seismic wave velocity measurements (SCPT). Over 80 pressuremeter (in soil) and dilatometer (in rock) profiles were performed. Numerous undrained shear strength profiles were developed with Nilcon vane shear tests in the cohesive soil.

Geophysical investigation consisting of P&S sonic waves and downhole tests were performed in 9 and 6 borings, respectively. The P&S method proved to be efficient to locate the fractured rock zones, as well as the numerous intrusive rocks intercepted by the borings.

In order to enhance recovery in the very dense till deposit and locate more precisely the interface between the till and the shale bedrock, a special drilling technique with the PQ3 core barrel having a specially designed diamond core bits were used to obtain, in one core run, almost intact sample of the till, fractured rock, and sound rock underneath. This technique proved to be very useful in establishing the limits between these geologic elements.

Rock core samples were inspected and logged by an experienced geologist. A detailed record of the rock structural descriptions, including condition, orientation, spacing, weathering and alteration of discontinuities, was performed and used for the determination of the Geological Strength Index (GSI) and Rock Mass Rating (RMR) used for foundation design. The CERCHAR test was also performed on rock samples to determine the Abrasiveness Index (CAI) using steel styluses with a Rockwell Hardness Scale (RHS) of 55.

Carrying out the subsurface investigation presented a unique challenge. Many borings required traffic control and overnight drilling. Over 80 SPT and CPT borings were drilled offshore with limited access to the river and very stringent environmental requirements (no sediment in water, biodegradable oil and fluids for drill rig, etc.), with the involvement of numerous agencies such as Transport Canada, St. Lawrence Seaway, Federal Bridge Agency, Hydro-Quebec, and others.

5 DRILLED SHAFT LOAD TESTING

In order to optimize the drilled shaft geotechnical design and allow the use of higher resistance values for axial capacity, two Osterberg-cell (O-cell) tests were performed on July 1st and August 25, 2015 by Loadtest USA on sacrificial drilled shafts at the West Abutment and at the Main Span Tower (MST). The purpose of the tests was to determine the design values of side and base resistance at the ultimate limit state on drilled shafts constructed using means and methods identical to those to be used on production foundations. Both tests yielded similar results. Brief description of the test results and analysis at the MST is described herein.

The construction procedure is described below in Section 9.3. The tested shaft diameter and depth were 1.18 m and 19.6 m respectively, with socket length of about 5 m. The tests were performed using one (1) 13.8 MN bidirectional embedded jacks (O-cell) to load the base area of the shaft against the side resistance of the socket above the base.

At the maximum load, the displacements above and below the O-cell were 4.81 mm and 12.85 mm, respectively. Those displacements corresponded to maximum downward and upward loads of 20.53

and 20.18 MN. Seven levels of two sister bar vibrating wire strain gages were attached diametrically opposed to the reinforcing cage, including four in the rock socket area below the steel casing.

The data showed the maximum unit skin friction and unit end bearing mobilized during the test along the rock socket were 1.6 and 32.4 MPa, respectively.

Typically, the design approach for side resistance relates the unit side resistance, f_s and the square root of the unconfined compressive strength of the bedrock, $\sqrt{q_u}$. The method contained in Turner (2006) is presented as equation (1):

$$f_s = C \cdot P_a \cdot \sqrt{\frac{q_u}{P_a}} \quad (1)$$

Where P_a is the atmospheric pressure (101 kPa), C is an empirical constant, and q_u is the unconfined compressive strength of the rock measured to be equal to 25 MPa at the load test location.

The CFEM (2006) recommends a range of values for the parameter C between 0.63 and 1.41 reflecting the variability of test results obtained by different authors, whereas AASHTO recommends the use of a value of 1, based on the most recent regression analysis of available load test data that is reported by Kulhawy et al. (2005).

One of the objectives of the load test was to calibrate the empirical parameter C against the results of the O-cell test, at the project site for shale. Based on the load test results, a value of C equal to 1 (consistent with AASHTO recommendations) was back-calculated from the equation.

The O-cell test results also showed that approximately 14 MN in end bearing was mobilized at the vertical displacement at which the maximum skin friction was mobilized (see Figure 5 below). Thus, approximately 23 percent of the total resistance were provided by the end bearing at displacements corresponding to maximum mobilized skin friction.

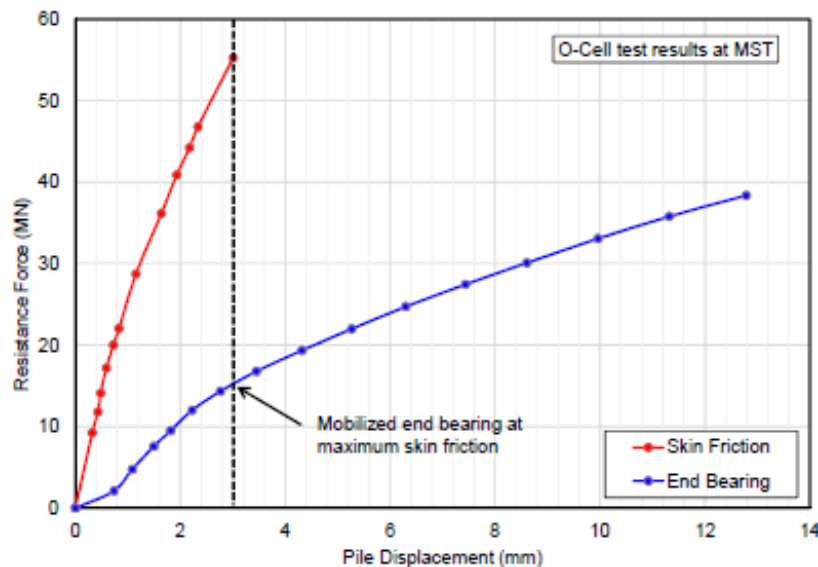


Figure 5. Skin friction and end bearing from O-cell test

The CFEM (2006) recommends the use of the Pells and Turner (1979) approach that is based on the theory of elasticity, to determine the load distribution between the end bearing and side shear. Using this approach, the tip resistance contribution would be approximately 12%. Therefore, the load tests showed the load transferred to the tip larger than that predicted by Pells and Turner approach, allowing the design to be optimized and resulting in a significant cost saving.

6 SAINT-PIERRE COLLECTOR PROTECTION

Widening of Highway 15 in Montreal was planned as a part of the project. Most of the widened part was to be constructed over an existing old collector called Saint-Pierre Collector (CSP), extending over 2.5 km between the Turcot Interchange and Gaetan-Laberge Boulevard. This combined sewer overflow discharges the sanitary sewage and storm water runoff to the Atwater Water Pollution Control Plant Treatment. The CSP is a double reinforced concrete culvert with an average height of 4.6 m. Figure 6 shows the CSP during construction in 1933. Since the structural condition of the CSP was unknown, the collector owner's requirement was not to increase the stress on the collector due to the new construction.

As a result, the geotechnical design for Highway 15 above the CSP was prepared in such a way that no additional load would be applied on the Collector. This was achieved by the compensating fill approach which consists of removing a portion of the existing fill and installing lightweight engineered fill material to the required grade such that the Collector experiences no increase in applied stresses. The lightweight fill used for this purpose was composed of expanded polystyrene (EPS) blocks. Since the cost of the EPS blocks per cubic meter is much higher than the regular earth fill material, and since the CSP extends over several kilometers along the project corridor, minimizing the use of EPS in the embankment would represent a large cost saving to the project.



Figure 6. Construction of Collector Saint-Pierre

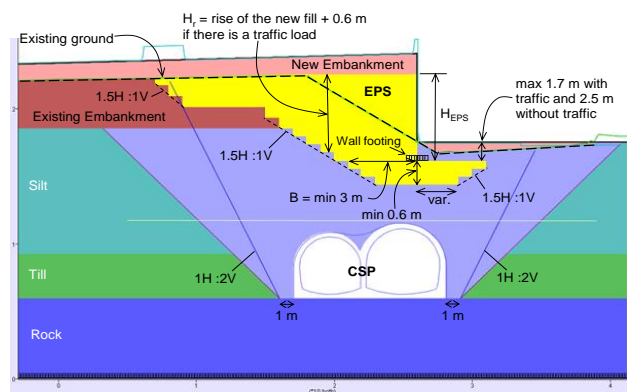


Figure 7. Typical EPS use for highway widening

Due to the complex geometry, the design and optimization of the EPS configuration over the CSP was investigated using numerical simulations conducted using a 2D finite difference program FLAC8.0. The purpose of the study was to determine the optimum influence zone of the collector beyond which any earthwork would have no stress increase on the collector. Figure 7 above is a typical representation of the use of EPS for the highway widening that results in no stress increase on the collector.

To accurately estimate the stresses induced by the new construction on the collector, staged construction was applied in the numerical analyses and a stress hardening soil model was used to account for soil under unloading and reloading conditions. Initial conditions were modeled as

horizontal layers of rock, till and fill material before building the CSP. Initial stresses were produced and followed by Plastic-Hardening analysis of the till layer. At the next stage, the collector and the backfill were built and then followed by another Plastic-Hardening analysis. The Plastic-Hardening model is a shear and volumetric hardening constitutive model used for the simulation of unloading-reloading situations. The existing embankment and retaining structures were then applied to the model and consequently stress and deformation analyses were performed by applying a 17.6 kPa traffic load. At the final construction stage, the planned new fill was analyzed, and the final predicted traffic load was applied.

The soil stiffness parameters were back-calculated based on in-situ settlement measurement performed at one of the retaining walls, designated as MS-1, located in the vicinity of the studied segment area. Settlement plates were installed, and settlement were recorded during the staged construction of the wall. The nonlinear modulus parameters of the soil were then calibrated by trial and error using FLAC. All stages of the MS-1 wall construction, including the initial condition, the excavation, and the wall layers were modeled in FLAC using the stage construction technique.

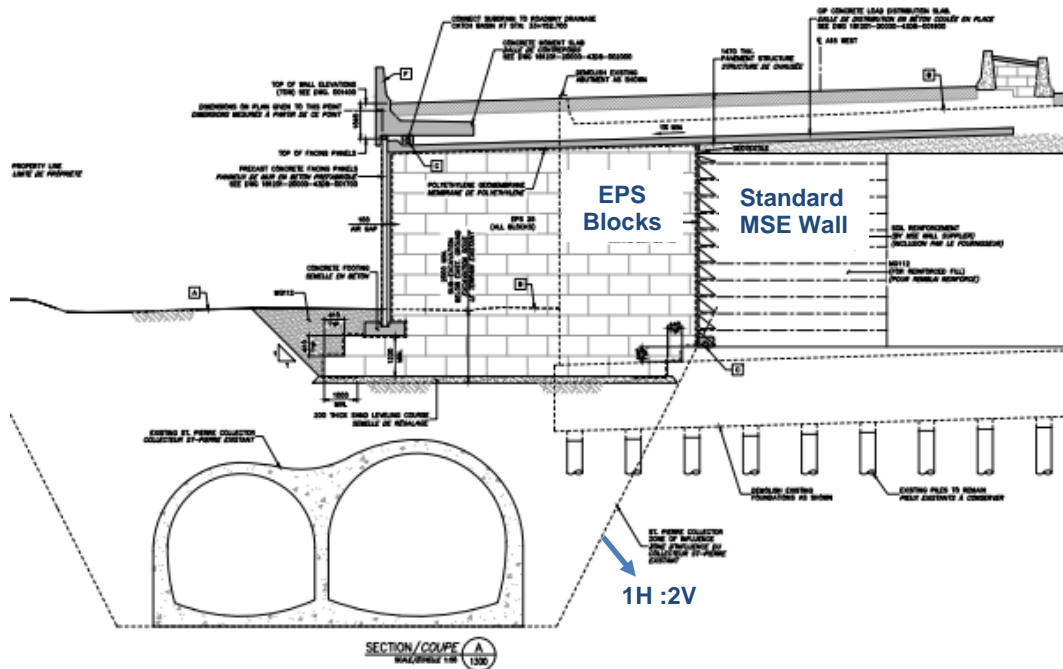


Figure 8. Use of EPS within the CSP zone of influence

Different configurations of EPS blocks were introduced into the model to determine the minimum EPS volume needed for each representative cross section in order to avoid applying any additional load on the CSP as a result of the new embankment.

The analyses showed that generally, any load applied on the surface outside of the 1H:2V lines did not have a significant effect on the horizontal and vertical stress on the collector.

Figure 8 above represents a typical use of EPS over the CSP. As shown, in this particular section, the existing highway was to be widened by over 15 m. Within the 1H:2V zone, part of the existing fill was excavated, and EPS was used as backfill material up to the proposed grade in order to not increase the

stress on the CSP. A standard Mechanically Stabilized Earth (MSE) wall was then constructed just behind the EPS and outside the zone of influence, to complete the highway widening.

The numerical simulation provided detailed information on the stress and deformation analysis of the cross section, as compared to analytical analysis, and helped reduce the project cost by over \$5M.

7 CONSTRUCTION OVER OLD LANDFILL

About 550 m long of the proposed Highway A15 between Gaetan-Laberge Blvd in Montreal and Ile des Sœurs (IDS) Bridge (See Figure 1 – Segment 2) was to be constructed along a new alignment where an old solid waste municipal landfill existed. The proposed highway profile was to be 2 to 7 m above the existing ground. Three single-span new bridges were to be constructed in this area. As a result of the poor soil conditions, these structures were to be founded on drilled shafts socketed into rock. Due to right-of-way limits, most of the new highway were to be supported by MSE Walls.

Over 25 borings were drilled in this area. The overburden consisted of heterogeneous fill material, up to 9 m thick, consisting of silt, sand and gravel with considerable amount of debris containing wood, steel, plastic, concrete, glass, metal, brick, garbage etc. The proportion of the debris was variable but could reach up to 90 percent in some zones within the fill. The underlying layer was a thin native glacial till soils underlain by the shale bedrock.

Several ground improvement techniques were discussed with the construction team (CJV) including:

- Over-excavation and replacement
- Dynamic compaction
- Vibro-compaction (or vibro-replacement)
- Column supported embankment
- Lightweight fill
- Preloading

Due to the thickness of the heterogeneous fill along proposed highway, replacement would not have been practical and could have been too costly and problematic due the contaminated nature of the material and the presence of groundwater.

The use of dynamic compaction or vibro-compaction to achieve a suitable bearing material would not have been effective due to the organic nature of the material and the presence of wood layers that could act as “springs” and prevent any increase in density of the underlying soils.

Column supported embankment that would transfer the entire embankment load to the underlying competent soil or rock, and/or the use of lightweight fill to minimize the applied load on the solid waste, would have been the best options. However, these two options are very costly. Therefore, CJV requested the design team to analyze the feasibility of the preloading option with phase construction.

A thorough analysis of the existing material properties was then conducted by the design team. The main geotechnical challenge was to estimate the strength and elastic parameters of the overburden needed to estimate the downdrag forces along the shafts of the three structures in this area, as well as the bearing capacity and settlement due to the placement of the new roadway fill on the heterogeneous fill.

Due to the nature of the debris material, the material properties could not be determined based only on the SPT N values. Therefore, SPTs were supplemented by pressuremeter tests to better predict the geotechnical properties and obtain more reliable estimate of the friction angle and the elastic properties. Over 25 pressuremeter tests were carried out in the area. The friction angle, ϕ , was estimated based on the following equation, proposed by Centre d'Études Ménard in 1970:

$$P_l = 2.5x2^{\frac{\phi-24}{4}} \quad (2)$$

Where P_l is the pressuremeter limit pressure.

Based on the above equation, a friction angle of 29 degrees was estimated for the debris layer.

In order to better assess the settlement behavior of this material a 7 m temporary embankment fill (causeway) was constructed across the landfill during the design phase. The causeway served also to allow traffic during the demolition and reconstruction of the existing IDS Bridge. To monitor the settlement of the causeway, a total of 32 settlement plates were installed along the causeway. The locations of the plates were selected as close as possible from boring locations to facilitate correlation with boring data.

All settlement plates showed mostly a clay-like behavior, as shown on Figure 9 below, which could be summarized as follows:

- “Primary” settlement, completed within 65 days
- “Secondary” settlement rates of about ± 0.55 mm/day.

A coefficient of “consolidation” c_v of $0.6 \text{ m}^2/\text{day}$ was then back-calculated from those results. A correlation between c_v and landfill thickness H was developed using exponential curve fitting technique and could be expressed by:

$$c_v = 0.08. e^{0.18H} \quad (3)$$

A secondary “consolidation” settlement rate, C_{α} of 0.15 was also back-calculated. The value of C_{α} was found to be independent from the landfill or roadway fill thicknesses.

Although the secondary settlement was a concern that would require regular maintenance and potentially grade raise during the project lifetime, preloading and phase construction was the selected ground improvement alternative for the embankment construction.

As a result, all wall construction was proceeded in two phases to allow settlement to occur prior to final construction. In the first stage, a wire faced MSE wall was constructed. In the second stage, the panel facing was installed. The first phase involved placing a surcharge corresponding to the total height of the wall plus the equivalent of 1.5 m (30 kPa) on the existing ground.

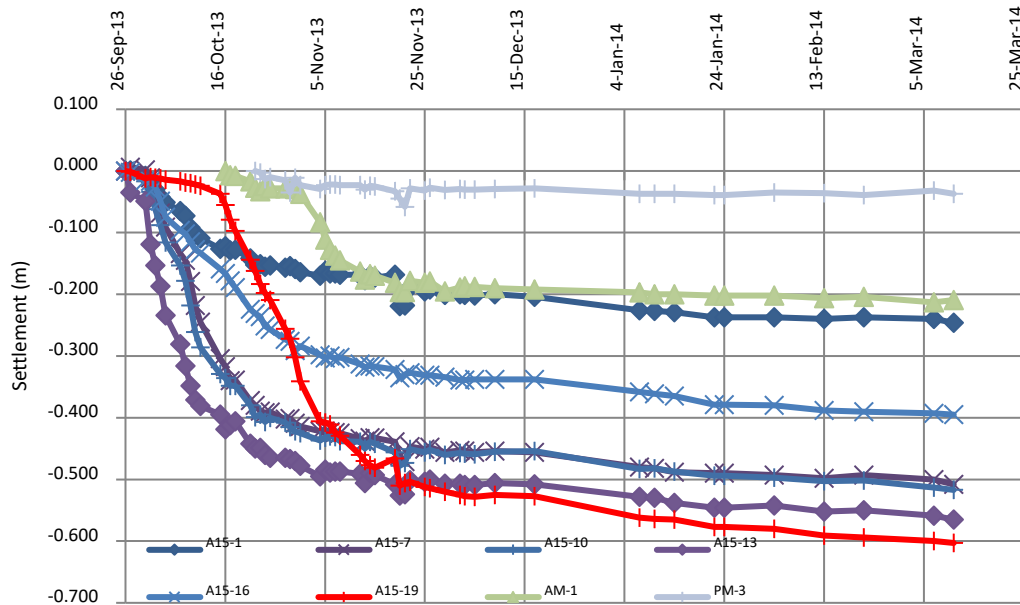


Figure 9. Typical settlement over time curves

At this stage settlement plates were installed during embankment construction to determine the magnitude and rate of settlement as describe in ASTM D6598. The settlement was monitored on weekly basis (twice a week) from the date of installation of the first device until the rate of settlement at each settlement plate was less than acceptable limits, generally less than 5 mm/week over two-week period. Then, in the second construction phase, the surcharge was removed, and construction was finalized by placing the facing 500 mm away from the front of the wall as well as the concrete barrier and the pavement on top of the wall. The 500 mm gap was then backfilled with BC 5-20 aggregate as specified in BNQ 2560-114. Figure 10 below illustrates the phase construction of one of the retaining walls designated as MS-R7.

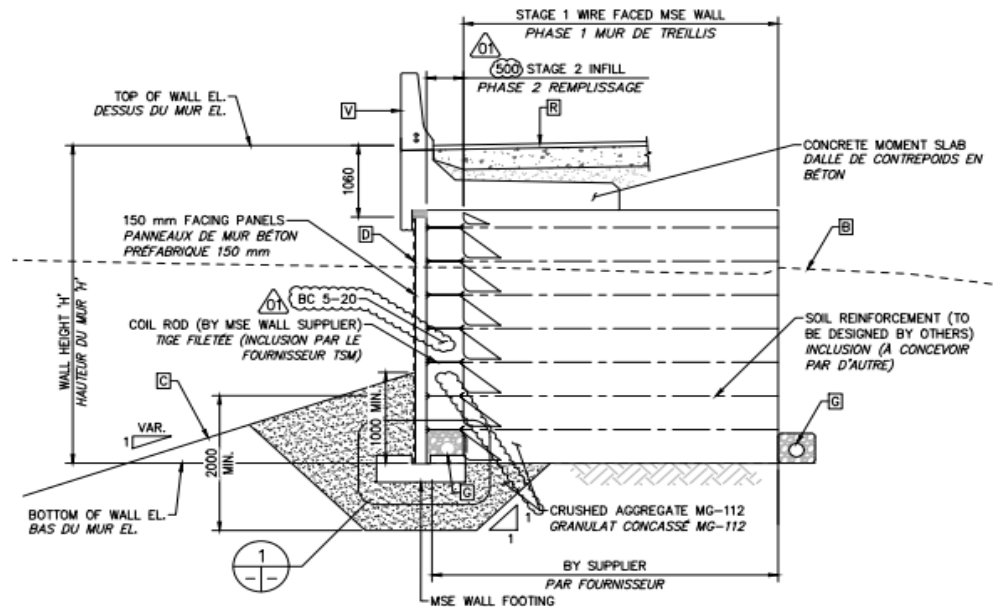


Figure 10: Staged construction of MSE Wall

The settlement magnitude and duration for the above mentioned 7 m height wall was about 150 mm and 6 months, respectively, consistent with the results obtained during the design phase.

8 DESIGN IN POTENTIALLY LIQUEFIABLE SOIL

Liquefaction triggering evaluations were performed for 2475-year, 975-year, and 475-year return periods based on simplified method proposed by Youd et al (2001). A design decision by the geotechnical team was made to consider the soil as liquefiable when the factor of safety was less than 0.9 and not susceptible to liquefaction for a factor of safety larger than 1.2. Numerous areas along the project alignment were found to be liquefiable including the soils at the “main” bridge West Abutment and at the East Abutment of IDS Bridge. For factors of safety between 0.9 and 1.2, the soil was considered as potentially liquefiable and required more detailed analysis. One such a case was the soil encountered between Wellington Street and Atwater Avenue in Montreal.

The subsurface conditions in this segment of the project consisted generally of fill material (silty sand) underlain by glacial till. In some areas, however, a silt layer was encountered between the fill and the till. The silt layer varied in thickness from about 2 to 8 m and had a density ranging from very loose to medium dense. The silt was estimated to be potentially liquefiable. Consequently, additional subsurface investigation was conducted mainly to determine the shear wave velocity, V_s profiles of the deposit using the seismic downhole method. Moreover, large soil samples were collected and sent to the University of Sherbrooke for detailed liquefaction analysis. The measured V_s in the field were utilized as references to reconstitute the laboratory soil samples to the same density as in the field. In other words, V_s tests performed at the site were used with laboratory measurements of V_s on the soil samples at different void ratios to reconstitute soil specimens at densities comparable to those experienced in the field. The samples were then subject to cyclic direct simple shear (DSS) test.

The tested silty soils had a plastic and liquid limit of 18 and 22 percent respectively, and an average clay content of 10 percent. Two specialized laboratory apparatuses were employed for this purpose: the piezoelectric ring-actuator technique (P-RAT) to measure V_s values of soil samples extracted from the site, and the TxSS seismic simulator to define the cycling shear resistance of soil samples and perform direct measurement of pore pressure.

Once the reconstituted samples were obtained, a series of strain-controlled undrained TxSS tests were performed to define the relationship between the cyclic shear strain (γ_{cyc}) and the applied number of cycles at a frequency of 4.0 Hz (close to the natural frequency of the deposit) until the soil liquefies. Initial liquefaction was defined as pore water pressure ratio, $R_u = \Delta u / \sigma'_c$ of 0.9, where σ'_c is the initial confining pressure and Δu is the excess pore pressure. The results for the reconstituted sample showed that liquefaction was likely to occur after 20 cycles.

In order to evaluate the cyclic resistance (CSR) according to the number of cycles, numerical modeling of the potentially liquefiable soil layers, using the computer code FLAC, was performed by applying directly earthquakes compatible with the Eastern Canada seismicity. First, a relationship between the energy dissipated during cyclic loading with the built up of the pore pressure was developed based on the TxSS tests for the tested soil. The dissipated energy per unit volume for a soil sample in cyclic loading was determined by integrating the area bound by stress–strain hysteresis loops. Second, this relationship was integrated into a dynamic response analysis through a constitutive law enabling it to

properly describe the hysteresis stress-strain behavior of the soil under consideration and making it possible to simulate the induced pore water pressure ratio R_u for any seismic loading and assess their potential liquefaction hazard.

Once the numerical model was calibrated, the shear distortions obtained numerically using FLAC and the SIMQKE ground motion at the depths where the soil samples were extracted, were applied to these samples in the seismic TxSS.

The analysis showed that seismic loading of the silty soil at the site would generate groundwater pressure in the order of 17% of the initial effective pressure. Hence the soils at the site were not susceptible to liquefaction under seismic loading for a return period of 2 percent in 50 years, although some reduction of strength would occur.

8.1 Drilled Shaft Design in Liquefiable Soil

By mutual agreement between the construction team (CJV) and the designers, increasing the shaft length and/or diameter was selected as the most viable and cost-effective method to address the negative impact of liquefaction on drilled shafts. Therefore, seismic design of foundations in liquefiable and potentially liquefiable soils took into consideration the additional forces induced by liquefaction on the foundations. The major effects of liquefaction on deep foundations are the loss of lateral support in the liquefied zone, ground settlement, and lateral spreading, which would result in downdrag load and additional lateral load on the deep foundations.

Foundations located in liquefiable soil, exhibiting a factor of safety of less than 0.9, were analysed for lateral spreading and downdrag. On the other hand, these two phenomena were assumed to be negligible for foundations located in the silty soil discussed above.

Occurrence of lateral spreading depends on the earthquake properties (magnitude and acceleration), site conditions (ground surface slope and thickness of the soil layer that is anticipated to liquify) and liquified soil conditions (grain size and percent fine.) The foundation would be loaded by a laterally displacing soil mass in conjunction with inertial loading from the superstructure. The liquefaction-induced lateral spreading was particularly investigated for the shafts near the shoreline at the IDS bridge East Abutment and the “main” bridge West Abutment. The lateral spreading demands were computed as the sum of the full passive soil pressure on the foundation and 50 percent of the inertial loading from the superstructure as suggested in Caltrans 2012.

The liquefaction-induced downdrag forces on shafts were also considered. The post liquefaction settlement was computed using the methodologies proposed by Wu and Seed (2004) using the $(N1)_{60}$ adjusted to a reference clean sand. The downdrag forces in the liquefying layer were then calculated using residual strength values estimated, as recommended by Caltrans (2012), using the Kramer and Wang (2007) equations.

Lateral resistance along drilled shafts were calculated using nonlinear p - y curves for soils and rock. Although several soil models are available in the literature to simulate the behavior of liquified soil, a design decision was made to assume, conservatively, a *total* loss of strength of the liquefiable soil. As for the silty soil discussed above, the increase of pore water pressure in the soil resulting from earthquake loading, although does not cause liquefaction, but will reduce the effective pressure and

hence its resistance. As a result, lateral resistance of the silty soil was adjusted (lowered) such that the p - y curve parameters were modified as follows Miyamoto (1987):

$$K_r = K_{max} \sqrt{(1 - R_u)} \quad (4)$$

$$P_{ur} = P_{u-max} (1 - R_u) \quad (5)$$

Where K_r and K_{max} are the reduced and static lateral subgrade reaction respectively; and P_{ur} and P_{u-max} are the reduced and static ultimate lateral resistance, respectively.

9 CONSTRUCTION CONSIDERATIONS

9.1 South Shore embankment construction

A 3 to 4 m thick Champlain Sea clay deposit was encountered on the South Shore approach roadway leading to the new bridge. The fill height to be placed on the existing ground to reach the proposed grade varied from 2 to 16 m with its maximum height at the east Abutment. The clay properties were determined from series of field and laboratory testing including vane shear and consolidation tests. The clay was of medium to high plasticity with average liquid limit and plasticity index of 45 and 27 percent, respectively; and an average water content of 38 percent. The average recompression and compression indices (C_r and C_c) were 0.02 and 0.6 respectively. Figure 11 shows the consolidation test results including the adopted design curve. The profiles of the effective stress and the preconsolidation pressure are shown on Figure 12 for 10 m high fill. The secondary compression index (C_{α}) was found to be approximately equal to 5 percent of C_c .

Several alternatives were studied to reduce the settlement to an acceptable level, including preloading and the use of lightweight fill. A detailed settlement analysis was performed for various embankment heights. Obviously, removing the entire clay layer to eliminate long term settlement would result in a massive and costly excavation. Partial removal of the clay layer would have a minimal effect on the total settlement. In fact, the influence of excavating 2 m of clay corresponds to a reduction in total settlement of only 20 mm for 10 m fill height. This is because the upper 1 to 2 m of clay (crust) is stiff with the softer soil being encountered on the lower part of the deposit. However, removing 1 to 2 m of clay would have a clear impact on settlement duration.

The most cost-effective option was the complete removal of the clay layer (4 m thick) at the east Abutment where the fill height is about 16 m and then gradually decrease the excavation depth with a transitional slope of 1:10 to a 1 m clay removal, followed by a gradual decrease of excavation thickness to zero.

Considering the impact that settlements can have on the construction schedule and the service life of the roadway, construction of the approach roadway was instrumented using 11 settlement plates installed at the bottom of the embankment between October 2015 (PT-01 to PT-05) and July 2016 (PT-06 to PT-14). Two lateral displacement pins were also installed at the base of the embankment slope and monitored. The total fill height was variable and reached 7 m in some locations.

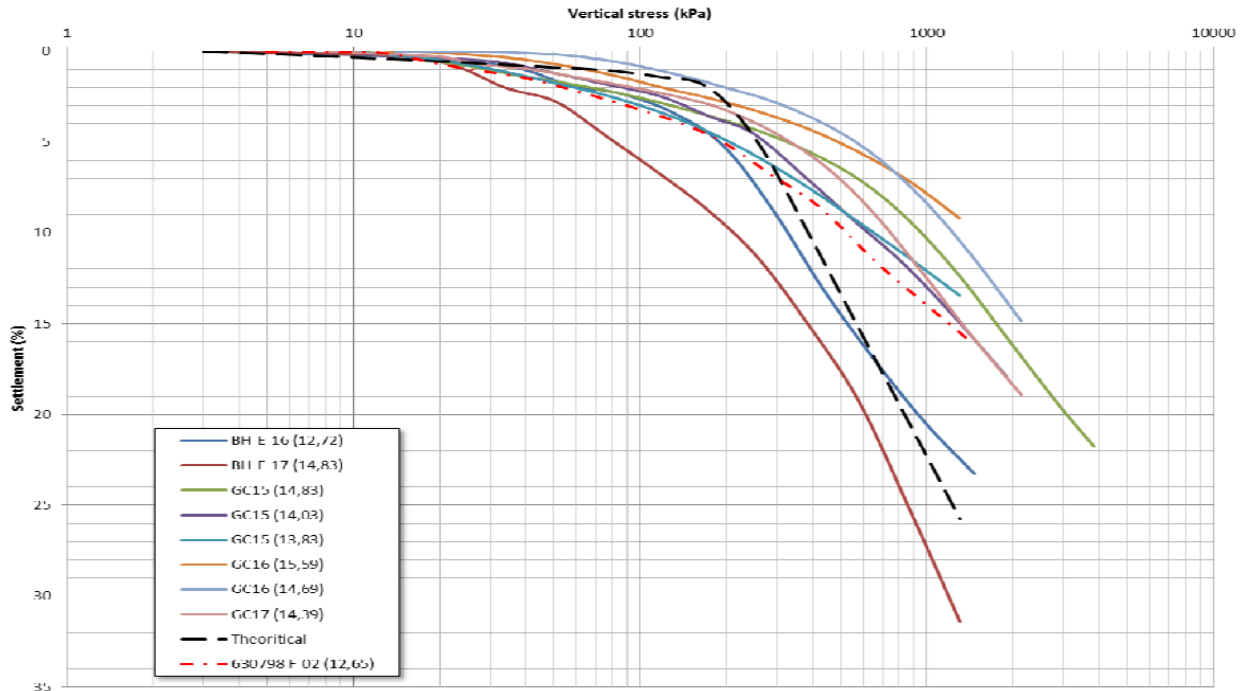


Figure 11. Consolidation test results

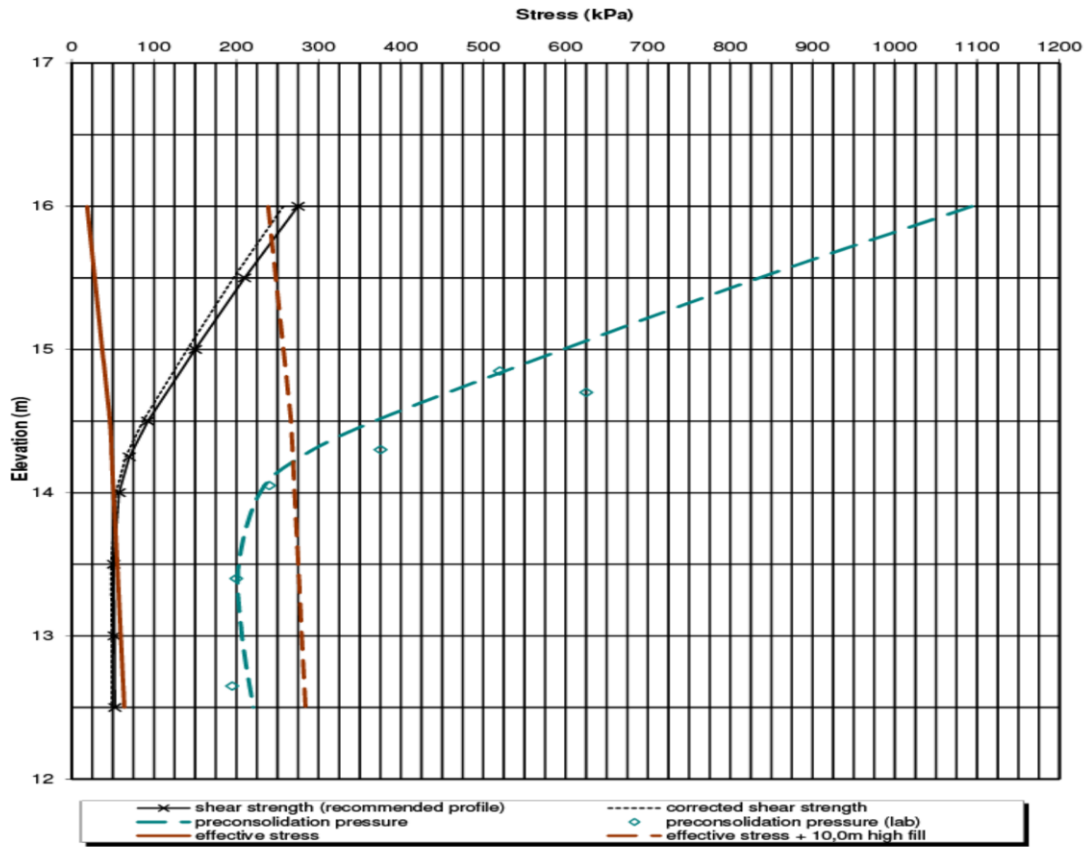


Figure 12. Effective stress and pre-consolidation pressure profiles

Results of measurements are presented on Figure 13. It was found that the measured settlements were larger than anticipated. For instance, the theoretical settlements for a 7 m fill height over a 3 m thick clay deposit were less than 30 mm, whereas the measured settlements reached between 80 and 180 mm. This can be explained by the difficulties in estimating the preconsolidation pressure from the consolidation curves that are “curved” without a clear break near the preconsolidation pressure and assessing accurately the consolidation behavior of the upper crust layer.

On the other hand, the measured consolidation time was at least 5 times faster than anticipated. Calculations were made using c_v measured in the softer clay while the upper crust layer is stiffer and oxidized and most likely more permeable, resulting in shorter consolidation time.

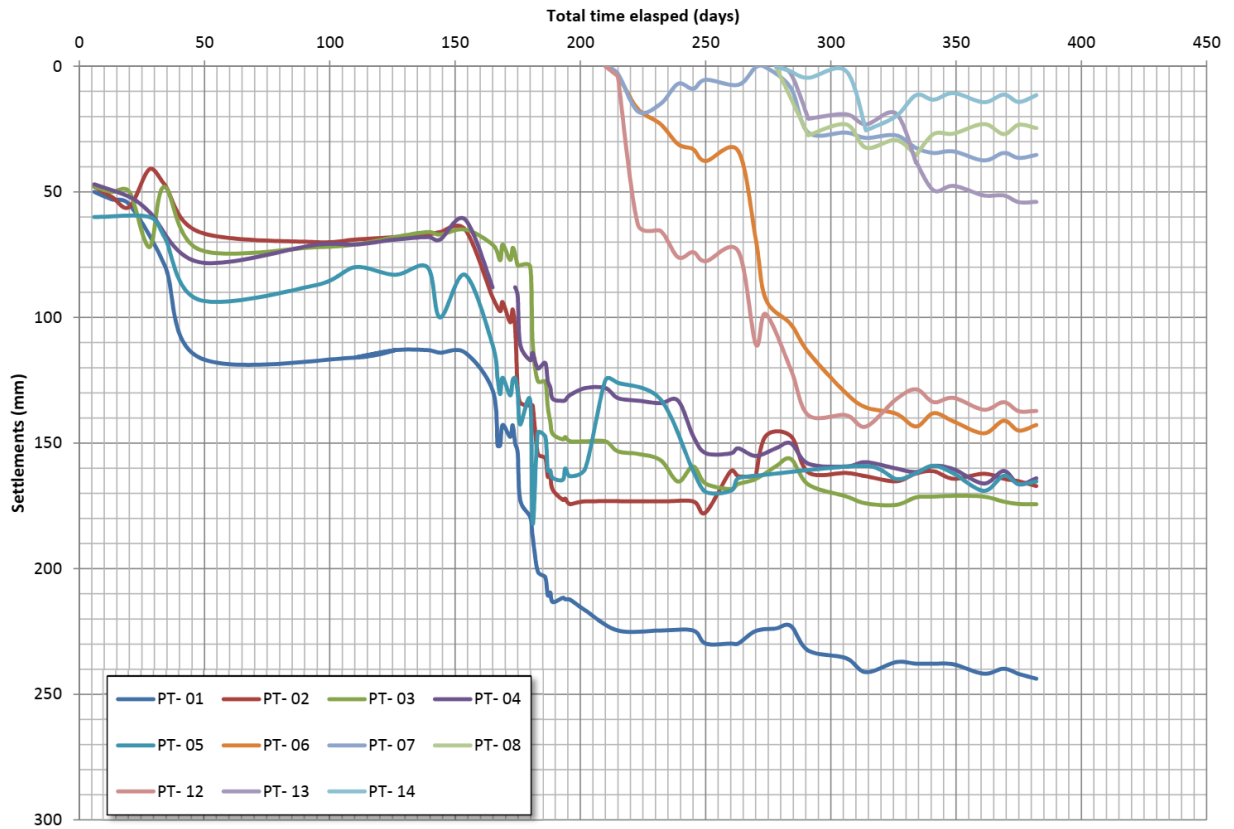


Figure 13. Field measured settlement

9.2 Spread footing

The construction of the spread footing of the offshore piers was done by excavating the soil and fractured rock to at least 300 mm below the predetermined foundation elevation. As shown on Figure 14 below, the excavation base was 1 m larger than the footing dimensions. The proposed side slope in the fractured rock was almost vertical whereas the till was excavated in a stair-like shape with 1 m bench and 0.6 m height and thus with an equivalent proposed slope of 1V: 1.7H. The purpose of the benching was to favor settling of the incoming sediments on the horizontal benches rather than in the bottom of the excavation.

The bottom of the excavation was first machine cleaned to ensure competent rock level had been reached. A more thorough cleaning using a sediment pump was performed immediately before the installation of the footing in order to remove the accumulated sediments at the base. It should be noted that although the excavation in some cases was left open for a few months before placing the footing, the potential of softening of the shale remained very low due to the fact that the excavation was always submerged.

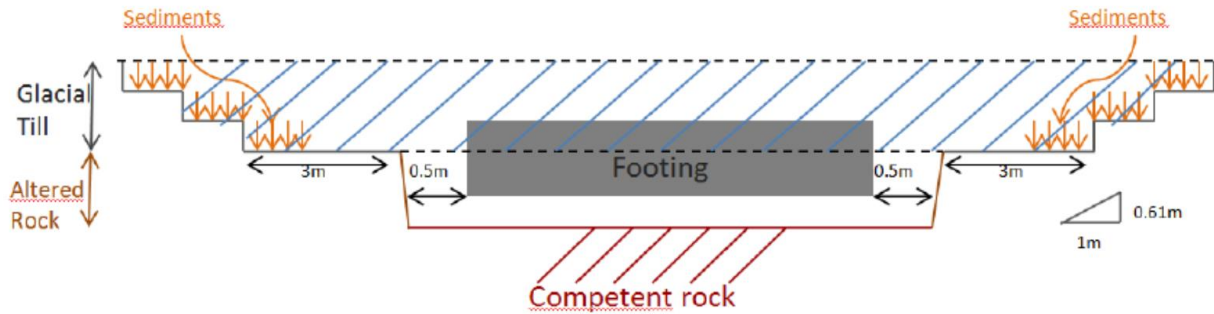


Figure 14. Excavated profile for spread footing

Immediately before placing concrete, the bottom of the excavation was once again inspected by the field geotechnical engineer using a sophisticated geo-camera to verify the quality of bearing stratum and the cleanout criteria.



Figure 15. Underwater foundation installation

The footing installation method consisted of lifting the prefabricated footing and placing it at the exact predetermined location on three hydraulic adjustable legs to ensure horizontal bottom of footing, as

shown on Figure 15 above. Once the footing was leveled in the right position, concrete was poured by tremie to fill the space between the rock and the footing.

9.3 Drilled Shaft

A hydraulic rig (LB 36-410) was used to insert a permanent steel casing through the overburden and the fractured rock until refusal on the rock surface was reached. The overburden was then excavated with an auger mounted on the drilling equipment.

Once the casing was sealed into rock, an auger and a bucket were used for drilling a slightly smaller shaft socket with a minimum of 300 mm of recess. To obtain a relatively flat base on the rock surface, the sub-contractor used a cleaning bucket (KBF-K) to flatten the surface.

The bottom and the rock socket walls of the shaft were cleaned with an airlift multiple time until the following cleanout criteria were met:

Maximum depth of sediment or any debris at any place on the base of the shaft not to exceed 40 mm.
Average depth of sediment is less than 15 mm of sediment at the time of concrete placement.

After cleaning the base, the frame was inserted into the excavation and was temporarily supported from the outer steel casing. Crosshole Sonic Logging (CSL) tubes were attached to the interior of the reinforcement cage. The tremie pipe was then placed through the tremie hole.

The concrete was pumped through a 5-inch diameter O.D. tremie line into the base of the shaft. During the concrete pouring, the volume of concrete in the pile was monitored as well as the volume that was poured from the delivery trucks combined with the concrete elevation which was measured on site directly into the shaft. The tremie pipe was held at least 3 meters in concrete at all times.

The constructed drilled shafts were subjected to multiple levels of quality control measures. Open shaft verticality through overburden soils was measured by the drilling rig alignment control and with the help of a 1.2 meters long spirit level for each shaft. This confirmed shaft verticality of the order of 0 - 2% was achieved. Once rock socket drilling was completed a Sub-Camera inspection device was used to confirm the rock socket base cleanliness using five spot sediment checking criteria.

Construction quality control involved concrete integrity testing using Ultrasonic Crosshole Testing (CSL) for all drilled shafts on the project. As for the "main" bridge, in addition to the CSL testing, Thermal Integrity Profiling (TIP) using sacrificial thermal wire cables to measure and monitor elevated concrete temperature during the hydration process of the concrete was also used to determine pile integrity. Any detected defect was assessed, and a remedial action was proposed.

9.4 Driven Piles

Closed end pipe piles driven to refusal on the shale bedrock were used for some substructures. As a result of the pile terminating on bedrock the design of the pile was based on the structural resistance of the pile.

It is well documented in the literature that some shales, particularly weathered shale, exhibit relaxation (decrease in resistance) phenomenon occurring during and after pile driving, generally

attributed to a release of locked in horizontal stresses (Thompson and Thompson, 1985). Hence, some practitioner engineers request the piles to be driven to a capacity (or pile penetration resistance) in excess of the required nominal resistance to account for the future loss of nominal resistance.

Thus, the nominal resistance was carefully assessed thorough dynamic testing program. The driving criteria was determined initially by running the wave equation program GRLWEAP and then confirmed by dynamic testing. Restrike was performed on all piles, a minimum of 3 days after initial driving. The piles were re-driven until the established termination criteria was reached. The vertical displacement occurring between the end of initial driving (EOID) and the end of restrike (EOR) was measured for all piles. Piles that exhibited displacement larger than about 3 mm were re-struck again until the measured displacement fell below the acceptable limit.

Dynamic tests were performed on selected piles at both the EOID and EOR, and in some cases at the beginning of restrike (BOR) in order to quantify time dependent changes in nominal resistance.

One example is the structure carrying Highway 15 over René-Lévesque Boulevard in Île-des-Soeurs (Nun's Island), designated as P11. A design load of 1750 kN was required. The results of GRLWEA program indicated that 31.2 kN drop hammer with 4.6 m stroke would be able to mobilize the nominal resistance of 3500 kN with stress levels below the minimum yield strength of 350 MPa at refusal conditions of 5 blows/1 mm.

The mobilized static resistance at the EOID for one of the piles on axis 1, based on the Case Method solution, was 3600 kN, exceeding the 3500 kN required. This was substantiated by signal matching analysis (CAPWAP) which indicated a nominal resistance of 3670 kN, with most of the resistance (3380 kN) carried by the toe. The nominal resistance at the BOR, based on the Case Method and CAPWAP solutions, was roughly 3100 kN, or 500 kN less than at the EOID, indicating large relaxation occurring between the EOID and BOR.

The pile was then re-driven until the required refusal criteria of 5 blows/1 mm was reached again. The measured vertical displacement to achieve the refusal criteria was 204 mm. A second re-drive of the pile was performed 3 days later where the displacement dropped to 58 mm. The third re-drive showed a displacement of less than 3 mm. At the end of the re-strike the mobilized resistance, as obtained by CAPWAP, had increased from 3670 kN to 3855 kN.

10 CONCLUSIONS

Replacement of the existing bridge across the St-Laurence River in Montreal posed significant geotechnical problems that were largely unsuspected prior to the geotechnical investigation and proposed bridge construction. The bridge had to be designed and constructed in a 42-month timeframe. The following concluding remarks could be made:

- The use of expanded polystyrene (EPS) blocks as lightweight fill along with numerical simulations for quantity estimate deemed very useful for the design optimization of the old collector protection.
- Staged construction was a cost-effective alternative to expansive ground improvements regarding the placement of the roadway embankment over an old solid waste municipal landfill.

- Laboratory cyclic shear tests conducted on potentially liquefiable soils helped determine the percentage loss of soil resistance and optimize the foundation seismic design.
- The O-Cell tests were a major contribution in optimizing the design of the drilled shafts socketed into shale.
- The use of dynamic testing (PDA and CAPWAP) at the EOID and EOR was very useful to assess the pile capacity with relation to relaxation phenomenon.
- Settlement monitoring of the clayey soil deemed necessary to capture the real consolidation behavior of the soil as compared to the theoretical analyses.

11 REFERENCES

1. AASHTO, 2014, *LRFD Bridge Design Specifications*, with Interims, American Association of State Highway and Transportation Officials, Seventh Edition, Washington, D.C., USA
2. Caltrans (California Department of Transportation) (2012). *Guidelines on Foundation Loading and Deformation Due to Liquefaction Induced Lateral Spreading*.
3. Karray, M. Hussien, M., and Chekired, M. 2016, *Characterization of the Dynamic Properties of Soils at the New Champlain Bridge Corridor Project Using the TxSS Seismic Simulator* University of Sherbrooke Report No. Geo-03-16, presented to SNC Lavalin.
4. MIYAMOTO, Y., 1987. *Pile Response During Earthquake and Performance Evaluation of Pile Foundation*, Kobori Research Complex, Kajima Corporation, Tokyo, Japan.
5. Thompson, C.D. and Thompson, D.E. (1985). *Real and Apparent Relaxation of Driven Piles*. American Society of Civil Engineers, Journal of Geotechnical Engineering, Vol. 111, No. 2, 225-237
6. Wu, J. and Seed, R.B. (2004). *Estimation of liquefaction- induced ground settlement (case studies)*, proceedings, Fifth International Conference on Case Histories in Geotechnical Engineering, New York.
7. Youd, T.L., Idriss, LM., Andrus, R.D., Arango, I., Castro, G., Christian, J.T., Dobry, R, Finn, W.D.L., Harder, L.F., Jr., Hynes, M.E., Ishihara, K., Koester, J.P., Liao, S.s.C., Marcuson III, W.F., Martin, G.R., Mitchell, J.K., Moriwaki, Y, Power, M.S., Robertson, PP.K., Seed, RB. and Stokoe II, K.H. (2001). Liquefaction Resistance of Soils: Summary Report from the 1996 NCEER and 1998 NCEER/INSF Workshops on Evaluation of Liquefaction Resistance of Soils. Journal of Geotechnical and Geoenvironmental Engineering, ASCE, 127(10): 817-833.